S. Weinbaum
Department of Mechanical Engineering,
City College of The City University
of New York,
New York, NY 10031

L. X. Xu
Department of Applied Sciences,
College of Staten Island/CUNY,
Staten Island, NY 10314

L. Zhu

A. Ekpene

Department of Mechanical Engineering,
City College of The City University
of New York,
New York, NY 10031

A New Fundamental Bioheat Equation for Muscle Tissue: Part I—Blood Perfusion Term

A new model for muscle tissue heat transfer has been developed using Myrhage and Eriksson's [23] description of a muscle tissue cylinder surrounding secondary (s) vessels as the basic heat transfer unit. This model provides a rational theory for the venous return temperature for the perfusion source term in a modified Pennes bioheat equation, and greatly simplifies the anatomical description of the microvascular architecture required in the Weinbaum–Jiji bioheat equation. An easy-to-use closed-form analytic expression has been derived for the difference between the inlet artery and venous return temperatures using a model for the countercurrent heat exchange in the individual muscle tissue cylinders. The perfusion source term calculated from this model is found to be similar in form to the Pennes's source term except that there is a correction factor or efficiency coefficient multiplying the Pennes term, which rigorously accounts for the thermal equilibration of the returning vein. This coefficient is a function of the vascular cross-sectional geometry of the muscle tissue cylinder, but independent of the Peclet number in contrast to the recent results in Brinck and Werner [8]. The value of this coefficient varies between 0.6 and 0.7 for most muscle tissues. In part II of this study a theory will be presented for determining the local arterial supply temperature at the inlet to the muscle tissue cylinder.

1 Introduction

In this paper a new simplified perfusion source term is derived to describe the effect of blood perfusion on local tissue heat transfer. Although this term is similar in form to the well-known Pennes source term, it differs fundamentally in concept since it describes the countercurrent thermal equilibration in a new primary vascular heat transfer unit, a muscle tissue cylinder surrounding secondary (s) vessels identified by Myrhage and Eriksson [23] as the basic anatomical structure in skeletal muscle in terms of vascular organization. This model thus combines the basic features of the Pennes perfusion source term and the Weinbaum–Jiji countercurrent heat exchange mechanism. The newly derived equivalent source term accurately describes the temperature difference between the countercurrent artery and vein and also relates this difference to the vascular geometry of the tissue cylinder. A substantial simplification of the anatomical description in the Weinbaum–Jiji approach is also possible since anatomical studies have shown that the vascular geometry of this new vascular heat transfer unit is common to nearly all skeletal muscle tissue.

The first quantitative relationship that described heat transfer in human tissue and included the effects of blood flow on tissue temperature on a continuum basis was presented by Pennes [20]. In this equation the effect of blood flow on tissue heat transfer was assumed to be equivalent to a heat sink or source whose strength is proportional to the volumetric perfusion rate and the arterial-venous temperature difference $T_a - T_v$. Three fundamental approximations in this equation have been questioned over the past decade: (i) T_v in this equation is unknown and has been approximated by the local tissue temperature T; (ii) T_a was approximated by the body core temperature rather than the local arterial supply temperature; and (iii) the local thermal equilibration, like gaseous exchange, occurred in the capillary beds and the small microvessels feeding these beds. Reasonable agreement between the theory and experimental results was obtained, although these fundamental approximations were never confirmed. The validity of the equation has been largely based on macroscopic thermal clearance measurements in which the adjustable free parameter in the theory, the blood perfusion rate, is chosen to provide reasonable agreement with experiments for the temperature decay in the vicinity of a constant temperature or pulsed overheat probe.

Applying a thermal equilibration length analysis, Chen and Holmes [12] showed that thermal equilibration occurred prior to the blood reaching the capillary beds. Later models by Weinbaum et al. [33] predicted that all thermally significant vessels in skeletal muscle were larger than 50 μm in diameter and occurred as countercurrent pairs. In 1985, Weinbaum and Jiji developed a new model equation for microvascular blood–tissue heat transfer and then applied this new equation to model peripheral tissue heat transfer [32]. Instead of attempting to modify the Pennes equation, they took a more fundamental physical approach, which related the local blood–tissue energy exchange to the local microvascular geometry and flow in the skeletal muscle. They found that in this tissue the predominant mode of heat transfer was the net heat loss to the tissue from the incomplete countercurrent exchange that took place between the paired vessels. The new Weinbaum–Jiji equation derived in [32] to account for this heat transfer mechanism showed that the thermal effect of the blood perfusion could be described in terms of a tensor conductivity k_{ijeff}, which was proportional to the square of the local Peclet number and dependent on the direction of the vessel axes relative to the local macroscopic tissue temperature gradient.

The Weinbaum–Jiji equation, like the Pennes equation, has several limitations in the derivation of the expression for k_{ijeff}: (i) It requires that the thermal equilibration between the artery–vein pairs not depart significantly from nearly perfect countercurrent exchange; (ii) it involves a detailed description of the branching microvascular geometry. The first limitation is usually satisfied in the muscle tissue at rest if the local vessels are less than 300 μm in diameter, but this maximum vessel size decreases rapidly as the flow rate is increased. The recent studies

Contributed by the Bioengineering Division for publication in the JOURNAL OF BIOMECHANICAL ENGINEERING. Manuscript received by the Bioengineering Division September 14, 1995; revised manuscript received June 5, 1996. Associate Technical Editor: R. B. Roemer.

by Zhu et al. [39] have shown that the criterion for the validity of the Weinbaum–Jiji equation, the ratio of the thermal equilibration length to the vessel length, $Le/L < 0.2$, breaks down for a maximally vasodilated tissue preparation with 200 μm diameter vessels. The first direct measurements of the thermal equilibration length in the countercurrent microvascular artery–vein pairs in Zhu et al. [38] show that this occurs when a Pe > 3 mm, where Pe is the Peclet number based on the vessel radius. The Weinbaum–Jiji equation can, therefore, not be applied without modification outside the peripheral tissue region for which it was first developed and even there the criterion for the validity of the equation can be violated at high flow rates in a 200 μm diameter artery–vein pair when Pe > 30. Limitation (*ii*) requires that detailed anatomical studies be performed to estimate the vessel number density, size, and artery–vein spacing for each vessel generation, as recently performed in Zhu et al. [39] for the rat cremaster muscle.

Many investigators have attempted to describe the effect of blood perfusion on local heat transfer and to elucidate the differences between the Pennes and Weinbaum–Jiji bioheat transfer models or to demonstrate experimentally which equation is more appropriate [1–5, 7–15, 18–19, 26–41]. Among those investigations, important insight into the different regions of validity of the Pennes and Weinbaum–Jiji models can be obtained by analyzing a more complex three-equation model for the artery, vein, and tissue and solving this system of equations for an idealized one-dimensional tissue geometry. Using a more rigorous three-equation model proposed by Baish et al. [4], Charny et al. [10] have compared the solutions of the three-equation model with the solutions of the Pennes equation and the Weinbaum–Jiji equation and concluded that the two approximate formulations are each appropriate in different tissue regions. The results for the three-equation model indicated that the Pennes equation is valid for vessels >500 μm diameter, where there is little countercurrent equilibration of the arterial supply temperature; whereas for 50–200 μm diameter vessels countercurrent convective heat exchange becomes increasingly important and the Weinbaum–Jiji equation is a more accurate description. This behavior has been confirmed by the detailed numerical calculations for a branching countercurrent network in Brinck and Werner [7].

One way to correct the Pennes equation is to introduce an "effectiveness factor" in the perfusion term by determining the net heat released from the countercurrent artery and vein to the surrounding tissue. This concept was first used by Chato [11] to investigate the thermal equilibration between countercurrent vessels in an infinite medium with a linear decrease in flow due to capillary bleed off. The ratio of the heat flow from the artery to the vein over a certain axial distance to the total heat flow in the artery is defined as "effectiveness" in Chato's paper. The axial variation of the artery and the vein temperature can be calculated considering the energy balance between the blood vessels. However, for an infinite medium this is a perfect heat exchange, since all the heat leaving the artery will eventually return to the vein. The "effectiveness" mentioned by Chato [11] is a measure of the capability of the artery to rewarm the countercurrent vein and is determined by the thermal resistance and mass transfer between the artery and the vein. Later, Wissler [34, 35] suggested that the only correction needed in the Pennes perfusion term was an "efficiency factor," which accounted for the fact that the venous return temperature and the tissue temperature might not be the same, even if the physical mechanism might not be precisely described by the Pennes model. In the statistical model presented by Baish [2], the most probable tissue temperature is 20 percent warmer than that predicted by Pennes equation if the isolated countercurrent vessels are spaced one diameter apart. This result implies an effectiveness of approximately 80 percent in the Pennes perfusion term. In the recent theoretical study by Brinck and Werner [8], they have used a spatially varying Pennes perfusion term to describe the radial temperature distribution between the core and surface in a human limb. Different efficiency factors are used in different regions, which are a function of vessel location and blood perfusion rate, and the values of the efficiency are determined by fitting the temperature distribution curve calculated from a three-dimensional vascular model [7]. While the concept of an efficiency factor is not new, in no previous study has a distinct anatomical structure been identified in which this concept could be applied to determine the local venous return temperature and hence the strength of a corrected Pennes source term.

Our new theoretical approach is divided into two parts. In part I, the present paper, a basic heat transfer anatomical structure is first identified that is common to all skeletal muscle tissue. The muscle tissue cylinder surrounding countercurrent vessel pairs (s) is analyzed and from this basic structure, the total heat released in the tissue cylinder is determined by calculating the temperature difference between the countercurrent artery and the vein at the inlet to the muscle tissue cylinder. Moreover, a closed-form expression for the "efficiency function" is derived from these principles and a relatively simple modified form of the Pennes perfusion source term is obtained. In part II of this paper, a theory will be presented for the local artery temperature by analyzing the thermal interaction in the larger countercurrent blood vessels that precede the s vessel tissue cylinders described herein.

2 Anatomical Background

In this paper a new theoretical framework is developed, which draws upon the essential features of both the Pennes and the

Nomenclature

a = vessel radius
a_v = ratio of the artery to the vein radius
C_f = specific heat of blood
k = thermal conductivity
l = vessel center to center spacing
L = half width of the muscle tissue cylinder
Pe = blood flow Peclet number
r = radial coordinate
R = radial coordinate
Re = Reynold number
R_t = dimensionless radius of the muscle tissue cylinder
s = vessel eccentricity
T_{ab0} = blood supply temperature at $z = 0$
T_{vb0} = venous return temperature at $z = 0$
T_{tlocal} = local tissue temperature at $R = R_t$
u = flow velocity component in the axial direction in the blood vessels
u_{a0} = average velocity component in the axial direction in the artery
$\vec{U}$ = dimensionless velocity vector in the tissue region
v = flow velocity component in the radial direction in the blood vessels
x, y = Cartesian coordinates
λ = eigenvalue
ρ_f = density
ϕ = polar angle in cylindrical coordinate
ϕ_{a-v} = angle between the artery and the vein

Subscripts

a = artery
b = bulk
f = fluid in vessels
h = homogeneous solution
p = particular solution
t = tissue
v = vein
$0 = z = 0$

Superscripts

$*$ = dimensional parameters

Weinbaum–Jiji model equations. The conceptual framework for this theoretical approach, first proposed in [28], has been developed from the comprehensive anatomical studies on the arrangement of the vascular bed in different types of skeletal muscles by Myrhage and Eriksson [23]. This study shows that the vascular arrangement bears close resemblance in various skeletal muscles. As shown in Fig. 1, the basic vascular unit in muscle tissue is a tissue cylinder of approximately 1 mm diameter that runs the length of the muscle and is roughly parallel to the surface of the muscle. Each muscle tissue cylinder consists of several hundred individual muscle tissue fibers of approximately 40 μm diameter and a parallel system of capillaries, which are fed by a periodically spaced transverse system of arteries and veins (t) that run perpendicular to the axis of the muscle tissue cylinder. The most important feature of this arrangement is that the basic muscle tissue cylinder is found to be the same whether it lies in deep or more peripheral tissue layers. This appears to be the best current model of the repetitive vascular organization in the skeletal muscle tissue.

A key insight in the new bioheat theory presented here is that the perfusion source term in the Pennes equation arises primarily from the heat released by the blood to the tissue as it transverses the length of each muscle tissue cylinder. The blood supply for the muscle tissue cylinder comes from a branching countercurrent network of supply vessels (SAV) that originate in the large axial vessels of the limb. The relatively short (1–3 mm) primary (P) arteries, which originate at periodic intervals from the SAV vessels, run obliquely across the muscle tissue cylinders and then branch into the long s vessels. The s vessels (50–100 μm in diameter) run along the axis of each muscle tissue cylinder. The length of the s vessels is determined by the spacing of the P vessels along the SAV vessels and is typically 10–15 mm. Each s vessel pair supplies a roughly periodic array of perpendicular t vessels (terminal arterioles that feed the capillaries) that radiate in all directions from the central axis of the tissue cylinder.

The spacing of the t vessels is the typical length of a capillary bed in the direction of the muscle fibers, 0.5–1.0 mm. In our model the t vessels are treated as a continuously distributed uniform bleed off through the walls of the s vessels, which can be viewed as porous cylinders. The s vessels are not perfect countercurrent heat exchangers and the perfusion source term arises from the net heat loss to the tissue from the vessel pair. The thermal equilibration occurs along the length of the thermally significant s vessels rather than in the t vessels, since the t vessels are typically 20–40 μm in diameter, and as shown in Weinbaum et al. [33, 18], are in thermal equilibrium with the local tissue. For all practical purposes, blood entering the t vessels from the s artery is at the vessel wall temperature of the s artery and blood returning to the s vein is similarly at its local wall temperature. This situation differs fundamentally from the blood entering or leaving the SAV vessel pair that supplies the P and s vessels where the arterial inlet and venous return temperatures both differ from the local tissue temperature.

Elementary thermal equilibration analysis [33] reveals that there is only a minor change in temperature along the P vessels because of their high Peclet number (20–100) and short length (1–3 mm), and the primary thermal equilibration is achieved through the countercurrent exchange that occurs along the length of the s vessels. Since there is little change in temperature along the P vessels, the local arterial supply and venous return temperatures (T_a and T_v) to the supply artery and vein (SAV) are effectively the same as the entrance temperature of the s vessels in the muscle tissue cylinder. Therefore, the boundary value problem for the muscle tissue cylinder can determine the venous return temperature and the local artery–vein temperature difference, in terms of the tissue cylinder geometry, Peclet number, and the local average tissue temperature T at the boundary of the tissue cylinder. This solution for the vessel temperature difference at the inlet of s vessels provides the long-sought-after expression for the perfusion source term in our modified Pennes equation.

The vascular ultrastructure sketched in Fig. 1 is a much more general description of skeletal muscle than the three-layer model for peripheral tissue proposed by the senior author in Weinbaum et al. [33] and Jiji et al. [18]. This three-layer model has been applied by several investigators to deep tissue and used to de-

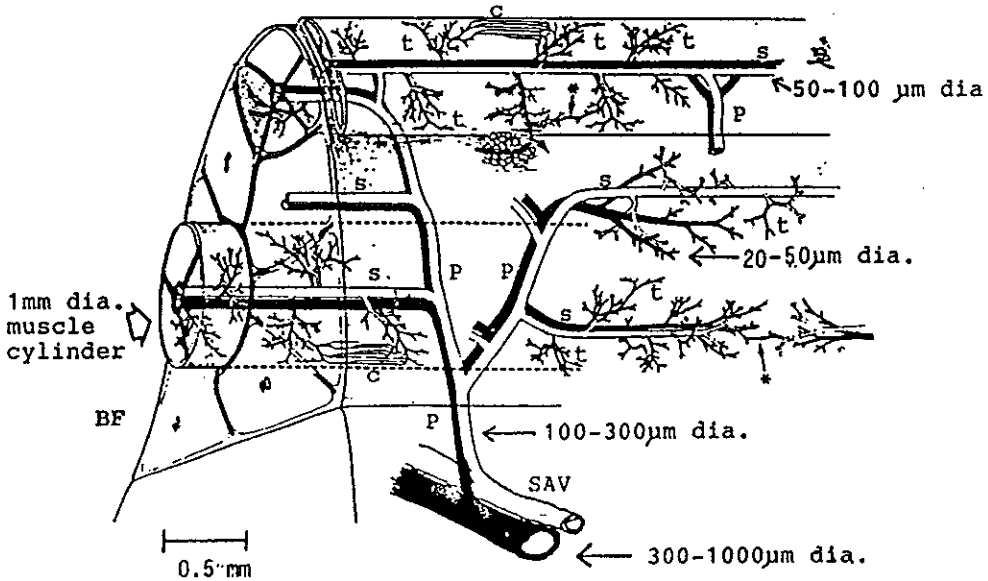

Fig. 1 Macro- and microvascular arrangement in the thin cat tenuissimus muscle (top of drawing) and the thick biceps femoris (BF). Terminal arterioles and venules (t), which are 20–40 μm in diameter, branch at a spacing of approximately 0.5 to 1 mm from the secondary vessels (s), which are 50–100 μm in diameter. The s vessels branch at about 1–2 mm from each other at equal intervals from the primary arteries and veins (P), which are 100–300 μm in diameter. The primary arteries and veins arise at a spacing of 1–2 cm from the main supply artery and vein (SAV), which are 300–1000 μm in diameter. Capillaries (c) are distributed throughout but are shown in only a few locations. From [23] with permission.

scribe heat transfer in an entire limb [7, 10, 36]. The key difference between the three-layer and the new conceptual model is the identification of an actual physiological structure in the new model, a muscle tissue cylinder surrounding s vessel pairs, which is a common fundamental unit for nearly all skeletal muscle tissue. In the three-layer model 8 to 10 generations of branching were identified with the largest vessels starting at the core of the limb. In [7, 10] a conceptually different tissue cylinder was introduced that is associated with periodically distributed vessel pairs, which diminish in size with each succeeding vessel generation [7, 10]. The peripheral tissue was assumed to start with vessels 300 μm diameter or smaller. These 300 μm vessels are actually the P vessels in Fig. 1 and it was not previously realized that the P vessels and their branchings to s and t vessels was a space filling repetitive arrangement that was present at all tissue depths.

Interest in modeling countercurrent vessels in perfused tissue and limbs has motivated several recent solutions for the heat transfer between two vessels embedded in a tissue cylinder [36, 41]. Wu et al. [36] presented a new analytic solution approach for treating any finite number of vessels arbitrarily positioned in a tissue cylinder with surface convection. Although the boundary conditions on the tissue cylinder in Fig. 1 differ from that in [36] and the blood vessels have axially varying velocities rather than a constant blood flow rate as in [36], it is possible to extend the analysis and obtain a closed-form expression for the venous return temperature of the s vessels and thus a new expression for the perfusion source term in a Pennes type bioheat equation.

3 Formulation

To derive the new perfusion source term, we first simplify the vascular architecture for the muscle tissue cylinder in Fig. 1 as shown in Fig. 2. The local arterial temperature at $z = 0$, the branching point of the s vessels from the P vessels, is T_{ab0}, and the unknown temperature of the blood returning to the P vein is T_{vb0}. Since the difference between T_{ab0} and T_{vb0} determines the total heat lost in the tissue cylinder, we seek a closed-form analytic expression for T_{vb0} as a function of T_{ab0}, the local tissue temperature ($T_{t\text{local}}$), the s vessel-tissue cylinder geometry, and the local perfusion rate.

Referring to Fig. 2, the principle simplifying assumptions of the model are: (*i*) Both the flow and temperature fields are quasi-steady on the time scale for the thermal equilibration of the tissue cylinder; (*ii*) the temperature at the outer radius R_t of the tissue cylinder is equal to the local tissue temperature $T_{t\text{local}}$, which is constant along the axial direction. This assumption is reasonable since the radius of the tissue cylinder R_t is much larger than the radii of the s vessels that run along its axis and this direction is roughly parallel to the skin surface (see assumption (*vi*)). Note the walls of the tissue cylinder are not adiabatic and the thermal energy that leaves the s artery can either pass through the boundary of the tissue cylinder or be recaptured by the returning s vein; (*iii*) the s vessels are part of an axial arcade, and at the midpoint between two P vessels ($z = L$), the blood velocity vanishes in both the axial artery and vein due to symmetry and continuity; (*iv*) the s vessels are viewed as long conduits with leaky walls and a uniform perfusion is assumed along the axial direction; (v) the radii of the s vessels do not vary in the axial direction and thus in view of (*iv*) the blood flow velocities vary linearly along the axis; (*vi*) axial conduction in the tissue cylinder is neglected. During exercise, when the blood flow rates are high, countercurrent flow is the dominant mode for axial thermal equilibration in comparison with axial conduction. When the blood flow rate is low, axial conduction will also be small since the s vessels run primarily parallel the skin surface rather than in the direction perpendicular to the skin surface in which the largest temperature gradient occurs. Considering that the length scale of the tissue cylinder (~6 mm) is usually much shorter than the characteristic length of temperature gradients produced during hyperthermia or through metabolism, large temperature gradients in the axial direction on the length scale L are unlikely; (*vii*) the temperature gradient $\partial T_{a,v}/\partial z$ in the convective term of the vessel energy equations can be approximated by the axial gradient of the vessel bulk temperatures, $dT_{ub,vb}/dz$, as previously justified in [41].

The nondimensional parameters and variables are defined as:

$$s_a = \frac{s_a^*}{a_a^*},\ s_v = \frac{s_v^*}{a_a^*},\ l = \frac{l^*}{a_a^*},\ r_a = \frac{r_a^*}{a_a^*},\ r_v = \frac{r_v^*}{a_a^*},$$

$$R = \frac{R^*}{a_a^*},\ R_t = \frac{R_t^*}{a_a^*},\quad z = \frac{z^*}{a_a^*},\ a_v = \frac{a_v^*}{a_a^*},\ L = \frac{L^*}{a_a^*},$$

$$\mathrm{Pe}_a = \frac{2\rho_f C_f a_a^* u_a}{k_f},\ u_v = \frac{u_v^*}{u_a^*},\ T_{a,v,t} = \frac{T_{a,v,t}^* - T_{t\text{local}}^*}{T_{ab0}^* - T_{t\text{local}}^*} \quad (1)$$

Here the subscripts a, v refer to the s artery and vein, and asterisks denote dimensional variables. a is the vessel radius and s is vessel eccentricity. All length variables are scaled by the artery radius, a_a^*. l is the vessel center to center spacing. R_t is the tissue cylinder radius. The basic geometry, symbols, and the coordinate system are sketched in Fig. 3.

The steady-state velocity field in the artery and the vein of the s vessel pair can be obtained by solving the Navier–Stokes equations for an incompressible fluid. As shown in the appendix, for a uniform bleed off rate from the s vessels, the inertia terms in the axial momentum equation are of $O(\mathrm{Re}_a a_a^*/L^*)$ times the viscous terms, and in the radial momentum equation the radial pressure gradient is of $O(L^{*2}/a_a^{*2})$. Thus, the motion in the radial direction is

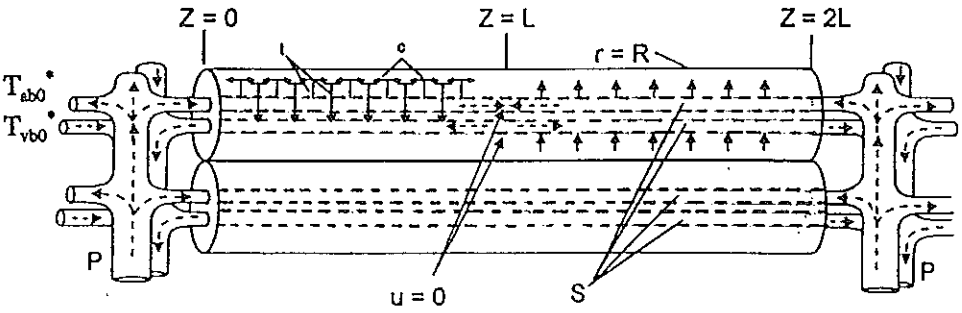

Fig. 2 Idealized model of the s vessel muscle tissue cylinder. Primary vessels (P) are shown at each end of a periodic unit in the s vessel arcade. At the location $z = L$, the blood flow velocity is equal to 0. While only two cylinders are shown, the tissue is filled with these repeating units as indicated by the branching of the P vessels.

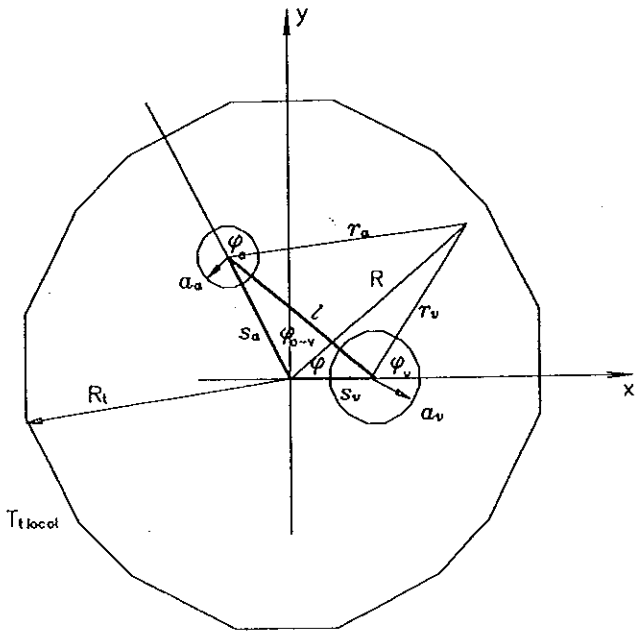

Fig. 3 The geometry of the cross-sectional plane and coordinate system in the muscle tissue cylinder

found to be much smaller than the motion in the axial direction. Since a_a^*/L^* is $O(10^{-2})$ and the Reynold number Re_a is at most $O(10)$, $Re_a a_a^*/L^* \ll 1$ and the governing equations for the velocity field can be greatly simplified. As shown in the appendix, the solutions for the velocity components in the axial and radial directions u_a^* and v_a^* in the artery are given by

$$u_a^* = 2u_{a0}^*\left(1 - \frac{z^*}{L^*}\right)\left(1 - \frac{r_a^{*2}}{a_a^{*2}}\right) \tag{2a}$$

$$v_a^* = \frac{u_{a0}^* a_a^*}{L^*}\left(\frac{r_a^*}{a_a^*} - \frac{r_a^{*3}}{2a_a^{*3}}\right) \tag{2b}$$

where u_{a0}^* is the average velocity at the entrance $z = 0$ of the s artery. Equations (2a) and (2b) apply downstream of a short entrance region, which for low Reynolds flow is less than two vessel diameters [16].

The dimensionless energy equation for the artery can be written as:

$$\frac{1}{r_a}\frac{\partial}{\partial r_a}\left(r_a\frac{\partial T_a}{\partial r_a}\right) + \frac{1}{r_a^2}\frac{\partial^2 T_a}{\partial \phi_a^2} = \mathrm{Pe}_a\left(1 - \frac{z}{L}\right)(1 - r_a^2)\frac{dT_{ab}}{dz}$$

$$+ \mathrm{Pe}_a\frac{1}{2L}\left(r_a - \frac{r_a^3}{2}\right)\frac{\partial T_a}{\partial r_a}, \quad r_a \le 1 \tag{3a}$$

One can show that the first term on the right side of this equation is $O(R_t)$ larger than the second term except as z approaches L where the first term vanishes. However, as will be shown later in the results section, one finds that the half length of the tissue cylinder L is larger than the thermal equilibration length. Thus, when z/L is near 1, thermal equilibration has already occurred, and both terms on the right side of Eq. (3a) vanish since there is no heat exchange between the vessels and the tissue. The second term can, therefore, be neglected for all z/L. One can draw the same conclusion for the vein following similar analysis. Introducing the above-given assumptions, the governing equations for the artery and the vein reduce to

$$\frac{1}{r_a}\frac{\partial}{\partial r_a}\left(r_a\frac{\partial T_a}{\partial r_a}\right) + \frac{1}{r_a^2}\frac{\partial^2 T_a}{\partial \phi_a^2} = \mathrm{Pe}_a\left(1 - \frac{z}{L}\right)(1 - r_a^2)\frac{dT_{ab}}{dz}, \quad r_a \le 1 \tag{2}$$

$$\frac{1}{r_v}\frac{\partial}{\partial r_v}\left(r_v\frac{\partial T_v}{\partial r_v}\right) + \frac{1}{r_v^2}\frac{\partial^2 T_v}{\partial \phi_v^2} = u_v\,\mathrm{Pe}_a\left(1 - \frac{z}{L}\right)\left(1 - \frac{r_v^2}{a_v^2}\right)\frac{dT_{vb}}{dz}, \quad r_v \le a_v \tag{3}$$

The tissue temperature field in the cross-sectional plane can be viewed as the temperature field generated by a line heat source–sink pair representing the s vessels in a porous media with convection. The velocity field $\tilde{U}$ satisfies Darcy's law and represents the flow through the t vessels and their subsequent branchings. This potential flow field due to the bleed-off from the s vessels can be approximated by the flow between an equal line source and sink located along the axes of the s vessels.

$$\nabla^2 T_t = \mathrm{Pe}_a\,\tilde{U}\cdot\nabla T_t, \quad R \le R_t \tag{4a}$$

One can show that the convective term generated by the capillary bleed off is of $O(R_t\,\mathrm{Pe}_a/2L)$ compared to the conduction term and thus, at least for resting conditions, insignificant in the tissue region. If one neglects the last term in Eq. (4a) and axial conduction, for the reason mentioned at the beginning of this section, the governing equation for the tissue region reduces to

$$\frac{1}{R}\frac{\partial}{\partial R}\left(R\frac{\partial T_t}{\partial R}\right) + \frac{1}{R^2}\frac{\partial^2 T_t}{\partial \phi^2} = 0, \quad R \le R_t, \quad r_a > 1, \quad r_v > a_v \tag{4}$$

The boundary conditions on the vessel walls are subtle. Since, as already noted, the thermal equilibration in the t vessels is almost instantaneous, the arterial and venous blood at the wall of the s vessels is the same as the tissue temperature at $r_a = 1$, and $r_v = a_v$ and the latter temperature is the same as the blood in the t vessels when it returns or exits the s vessel pair. Therefore,

$$T_a = T_t, \quad r_a = 1$$

$$T_v = T_t, \quad r_v = a_v \tag{5}$$

For the energy flux both diffusive and convective fluxes must be considered,

$$\frac{\partial T_a}{\partial r_a} + \mathrm{Pe}_a\frac{v_a^*}{u_{a0}^*}T_a|_{r_a=1} = \frac{\partial T_t}{\partial r_a} + \mathrm{Pe}_a\frac{\tilde{U}^*}{u_{a0}^*}T_t|_{r_a=1}$$

$$\frac{\partial T_v}{\partial r_v} + \mathrm{Pe}_a\frac{v_v^*}{u_{a0}^*}T_v|_{r_v=a_v} = \frac{\partial T_t}{\partial r_v} + \mathrm{Pe}_a\frac{\tilde{U}^*}{u_{a0}^*}T_t|_{r_v=a_v} \tag{6a}$$

However, from continuity $v_a^* = \tilde{U}^*$ and $v_v^* = \tilde{U}^*$ at $r_a = 1$ and $r_v = a_v$, respectively, and $T_a = T_t$, $T_v = T_t$. Thus, Eq. (6a) reduces to

$$\frac{\partial T_v}{\partial r_a} = \frac{\partial T_t}{\partial r_a}, \quad \text{at} \quad r_a = 1$$

$$\frac{\partial T_v}{\partial r_v} = \frac{\partial T_t}{\partial r_v}, \quad \text{at} \quad r_v = a_v \tag{6}$$

Finally, the boundary condition on the tissue cylinder surface is given by

$$T_t = 0, \quad \text{at} \quad R = R_t \tag{7}$$

Note that boundary condition (7) is essential to the analysis since it requires the blood to equilibrate to the local tissue temperature in the small vessels. If an adiabatic or periodic boundary condition was applied at R_t there would be no net heat loss through the boundaries of the tissue cylinder and one would end up with the trivial result that $T_{vb0} = T_{ab0}$. In Eqs. (2) and (3), T_{ab} and T_{vb} are artery and vein bulk temperatures, respectively. These bulk temperatures are defined as

$$T_{ab} = \frac{2}{\pi}\int_{-\pi}^{\pi}\int_{0}^{1} T_a(1 - r_a^2) r_a dr_a d\phi_a \tag{8}$$

$$T_{vb} = \frac{2}{\pi a_v^2}\int_{-\pi}^{\pi}\int_{0}^{a_v} T_v\left(1 - \frac{r_v^2}{a_v^2}\right) r_v dr_v d\phi_v \tag{9}$$

4 Solution for Countercurrent Flow

A theoretical solution to the complicated boundary value problem summarized in the last section can be obtained by modifying the solution procedure outlined by Wu et al. [36]. The simplifications introduced in the governing Eqs. (2), (3), and (4), and the boundary conditions enable us to separate variables and solve the boundary value problem in the cross-sectional plane independent of that in the axial direction. Using this approach, the axial interaction between vessels is reduced to a coupled system of ordinary differential equations for the axial bulk temperature variation in each vessel.

The solution for the temperature in the artery, the vein, and the tissue is decomposed into a particular solution and a general solution. They are expressed as:

$$T_a = \left(r_a^2 - \frac{1}{4}r_a^4 - \frac{3}{4}\right)\frac{\mathrm{Pe}_a}{4}\left(1 - \frac{z}{L}\right)\frac{dT_{ab}}{dz} + \frac{\ln (r_v/a_v)}{4} a_v^2 u_v \mathrm{Pe}_a\left(1 - \frac{z}{L}\right)\frac{dT_{vb}}{dz} + T_h \tag{10}$$

$$T_v = \left(r_v^2 - \frac{1}{4}\frac{r_v^4}{a_v^2} - \frac{3}{4}a_v^2\right)\frac{u_v \mathrm{Pe}_a}{4}\left(1 - \frac{z}{L}\right)\frac{dT_{vb}}{dz} + \frac{\ln r_a}{4}\left(1 - \frac{z}{L}\right)\frac{dT_{ab}}{dz} + T_h \tag{11}$$

$$T_t = \frac{\ln r_a}{4}\mathrm{Pe}_a\left(1 - \frac{z}{L}\right)\frac{dT_{ab}}{dz} + \frac{\ln (r_v/a_v)}{4} a_v^2 u_v \mathrm{Pe}_a\left(1 - \frac{z}{L}\right)\frac{dT_{vb}}{dz} + T_h \tag{12}$$

where T_h, the homogeneous solution in the three regions, is given by

$$T_h = \left\{[b_0 + \sum_{n=1}^{\infty} b_n R^n \cos[n(\phi - \phi_{a-v})]]\frac{dT_{ab}}{dz} + [c_0 + \sum_{n=1}^{\infty} c_n R^n \cos[n\phi]] a_v^2 u_v \frac{dT_{vb}}{dz}\right\}\mathrm{Pe}_a\left(1 - \frac{z}{L}\right) \tag{13}$$

The solutions (10)–(12) for the blood vessels and the tissue satisfy matching conditions (5) and (6) on the vessel surfaces. Using contour integrations and residue theory as outlined in the appendix of Wu et al. [36], one can obtain closed-form expressions for the coefficients b_n and c_n by applying the boundary condition at $R = R_t$

$$b_0 = (-\ln R_t)/4 \tag{14}$$

$$c_0 = [-\ln (R_t/a_v)]/4 \tag{15}$$

$$b_n = s_a^n/(4nR_t^{2n}), \quad n = 1, 2, \ldots \infty \tag{16}$$

$$c_n = s_v^n/(4nR_t^{2n}), \quad n = 1, 2, \ldots \infty \tag{17}$$

The temperature solutions in the artery and vein are now used to determine the bulk temperatures T_{ab} and T_{vb}. Substituting Eqs. (10) and (11) into Eqs. (8) and (9) and evaluating the double integrals, one can relate the vessel bulk temperatures to their gradients:

$$T_{ab} = \left\{A_{11}\frac{dT_{ab}}{dz} + A_{12}\frac{dT_{vb}}{dz}\right\}\left(1 - \frac{z}{L}\right)\mathrm{Pe}_a \tag{18}$$

$$T_{vb} = \left\{A_{21}\frac{dT_{ab}}{dz} + A_{22}\frac{dT_{vb}}{dz}\right\}\left(1 - \frac{z}{L}\right)\mathrm{Pe}_a \tag{19}$$

where $A_{11\sim22}$ are functions of the local vascular geometry only. Applying the summation equality,

$$\sum_{n=1}^{\infty}\frac{p^n}{n}\cos(n\phi) = -\tfrac{1}{2}\ln(1 - 2p\cos\phi + p^2), \quad |p| < 1$$

one obtains compact and easy-to-use expressions for the $A_{11\sim22}$:

$$A_{11} = \left[\sum_{n=0}^{\infty} b_n s_a^n - \frac{11}{96}\right] = -\frac{1}{4}\left\{\ln\left[R_t\left(1 - \frac{s_a^2}{R_t^2}\right)\right] + \frac{11}{24}\right\} \tag{20a}$$

$$A_{12} = \left[\sum_{n=0}^{\infty} c_n s_a^n \cos(n\phi_{a-v}) + \frac{\ln (l/a_v)}{4}\right] a_a^2 u_v = -\frac{a_v^2 u_v}{4}\ln\left[\frac{R_t}{l}\sqrt{1 - \frac{2s_a s_v}{R_t^2}\cos\phi_{a-v} + \frac{s_a^2 s_v^2}{R_t^4}}\right] \tag{20b}$$

$$A_{21} = \left[\sum_{n=0}^{\infty} b_n s_v^n \cos(n\phi_{a-v}) + \frac{\ln (l)}{4}\right] = -\frac{1}{4}\ln\left[\frac{R_t}{l}\sqrt{1 - \frac{2s_a s_v \cos\phi_{a-v}}{R_t^2} + \frac{s_a^2 s_v^2}{R_t^4}}\right] \tag{20c}$$

$$A_{22} = \left[\sum_{n=0}^{\infty} c_n s_v^n - \frac{11}{96}\right] a_v^2 u_v = -\frac{a_v^2 u_v}{4}\left\{\ln\left[\frac{R_t}{a_v}\left(1 - \frac{s_v^2}{R_t^2}\right)\right] + \frac{11}{24}\right\} \tag{20d}$$

The coupled equations (Eqs. (18) and (19)) for the vessel bulk temperatures are linear, ordinary differential equations that can be solved once the appropriate boundary conditions in the axial direction are specified. For countercurrent flow, these boundary conditions are the prescribed bulk temperatures at the inlets of the vessels. The arterial inlet temperature $T_{ab}(0)$ is always equal to 1, while the venous inlet temperature at $z = L$ is equal to the tissue temperature, i.e., $T_{vb}(L) = 0$. The latter assumption is reasonable, since at $z = L$ the flow is zero and one has achieved thermal equilibration between the vessels and the tissue since the countercurrent flow is the only driving force for the local axial temperature gradient.

The general solution of Eqs. (18) and (19) is an eigenfunction of the form $(1 - z/L)^{\lambda_i}$, where the eigenvalue λ_i can be

negative, positive or a complex variable, and T_{ab} and T_{vb} are arbitrary combinations of all possible eigenfunctions. Of the two real eigenvalues (complex eigenvalues are physically impossible for this application), one is positive (λ_1) and the other is negative (λ_2). Due to the boundary conditions mentioned above, one can exclude the eigenfunction with negative eigenvalue (λ_2). Therefore, the solutions of Eqs. (18) and (19) are given by

$$T_{ab} = (1 - z/L)^{BL/\mathrm{Pe}_a}$$
$$T_{vb} = T_{vb0}(1 - z/L)^{BL/\mathrm{Pe}_a} \tag{21}$$

where

$$B = \frac{(A_{11} + A_{22}) + \sqrt{(A_{11} + A_{22})^2 - 4(A_{11}A_{22} - A_{12}A_{21})}}{-2(A_{11}A_{22} - A_{12}A_{21})} \tag{22a}$$

$$T_{vb0} = -\frac{1}{BA_{12}} - \frac{A_{11}}{A_{12}} \tag{22b}$$

$$\Delta T = T_{ab0} - T_{vb0} = 1 - T_{vb0} = 1 + \frac{1}{BA_{12}} + \frac{A_{11}}{A_{12}} \tag{22c}$$

It is clear that the eigenvalue λ_1 is proportional to the cylinder length L and inversely proportional to the flow Peclet number. However, the venous return temperature T_{vb0} is only a function of the parameters $A_{11} \sim A_{22}$ and the latter depend only on the local cross-sectional geometry. T_{vb0} is thus independent of the flow Peclet number and the tissue cylinder length L.

If there is no bleed off ($L \to \infty$), the expressions for T_{ab0} and T_{vb0} will become

$$T_{ab} = e^{-Bz/\mathrm{Pe}_a}$$
$$T_{vb} = T_{vb0}e^{-Bz/\mathrm{Pe}_a} \tag{23}$$

where the coefficient B and T_{vb0} are still given by Eqs. (22a) and (22b). The thermal equilibration length for both the artery and the vein will be Pe_a/B. The presence of the t vessel bleed off from the s vessels thus changes the nature of the solution from an exponential to a power law decay.

5 The New Modified Perfusion Source Term and Bioheat Equation

The dimensionless temperature difference between the vessels at the entrance of the tissue cylinder, $\Delta T = (T_{ab} - T_{vb})|_{z=0} = 1 - T_{vb0}$, is the key parameter that determines the average heat loss per unit volume (q_f, W/m^3) inside the tissue cylinder. It is given by

$$q_f\,(\mathrm{W/m^3}) = \frac{\rho_f C_f \pi a_a^{*2} u_a^* (T_{ab0}^* - T_{vb0}^*)}{\pi R_t^{*2} L^*} \tag{24}$$

Introducing the definition of volumetric perfusion rate, $w_f = (\pi a_a^{*2} u_a^*)/(\pi R_t^{*2} L^*)$, and the dimensionless temperatures, one can rewrite expression (24) as

$$q_f(\mathrm{W/m^3}) = \rho_f C_f w_f \Delta T(T_{ab0}^* - T_{\mathrm{local}}^*) \tag{25}$$

where ΔT is given by Eq. (22c). If one substitutes the modified perfusion source term expressed by Eq. (25) and the metabolic source term q_m into the conventional heat conduction equation, one obtains a modified form of the Pennes equation,

$$\rho_t C_t \frac{\partial T_t^*}{\partial t} = \nabla k_t \nabla T_t^* + \rho_f C_f w_f \Delta T(T_{ab0}^* - T_t^*) + q_m \tag{26}$$

Expression (25) for the countercurrent perfusion source term is similar to the Pennes perfusion term except that there is a correction coefficient, ΔT, given by Eq. (22c), which accounts for the fact that the venous return temperature T_{vb0} is not the local average tissue temperature. ΔT is equivalent to a heat exchanger effectiveness and plays the same role as the efficiency function introduced in [8] except that one is dealing with a different concept for the tissue cylinder and, as we show below, ΔT is independent of the flow and depends only on the muscle tissue cylinder geometry in contrast to the results in [8] where ΔT is a function of Pe.

To simplify the expression for the venous return temperature, we consider the case of equal size blood vessels symmetrically positioned relative to the cylinder center, i.e., $a_v = 1$, and $s_a = s_v$. If the mass flow in each vessel is the same ($a_v^2 u_v = -1$), the A_{ij} coefficients in Eqs. (20a–d) reduce to

$$A_{11} = -A_{22} = -\frac{1}{4}\left\{\ln\left[R_t\left(1 - \frac{s_a^2}{R_t^2}\right)\right] + \frac{11}{24}\right\} \tag{27a}$$

$$A_{12} = -A_{21} = \frac{1}{4}\ln\left[\frac{R_t}{l}\sqrt{1 - \frac{2s_a^2\cos\phi_{a-v}}{R_t^2} + \frac{s_a^4}{R_t^4}}\right] \tag{27b}$$

The final form of the correction coefficient ΔT thus simplifies for an artery and vein of equal size to

$$\Delta T = 1 + \frac{A_{11}}{A_{12}} + \sqrt{\frac{A_{11}^2}{A_{12}^2} - 1} \tag{28}$$

Here A_{11} and A_{12} are given by Eqs. (27a) and (27b), respectively. Equation (28) shows that ΔT involves only two coefficients which are easily calculated.

6 Results

From this analysis, the correction coefficient ΔT is only a function of the vascular geometry of the muscle tissue cylinder. The parameters needed to calculate ΔT are the ratio of the tissue cylinder radius to the artery radius, R_t, and the relative locations of the countercurrent vessel pair in the cross-sectional plane. Several investigators [6, 17, 20–24] have described the vascular arrangements of various skeletal muscles and have measured the dimensions of the intramuscular vessels and the muscle tissue cylinder. These measurements are summarized in Table 1. Usually, the radius of the secondary artery is about 25–50 μm and the corresponding values for the venous vessels are about 50 percent larger. The tissue cylinder radius is approximately between 500–1000 μm. For different skeletal muscles, these values may vary, but the ratio of the tissue cylinder radius to the artery radius of different muscles in Table 1 does not vary greatly and the mean value of R_t is approximately 20. Thus, for other skeletal muscles that are not listed in this table, one expects to obtain similar values for R_t. Anatomic studies show that the s vessels are closely spaced countercurrent vessels, which are located near the center of the tissue cylinder. Therefore, in this paper, we assume the countercurrent pair has small eccentricity in the tissue cylinder and the vessel center to center spacing varies from 2 (touching configuration) to 6.

The blood flow Peclet number in the s artery (50–100 μm dia) can vary from 5 (resting state) to 50 (exercise). Figure 4 shows how this blood flow Peclet number variation influences the axial temperature variations in the vessels for a fixed L. One notes that the axial variation of the vessel bulk temperatures is significantly altered by changing the Peclet number. However, the venous return temperature at $z = 0$ is independent of Pe_a. In section 3, we assumed that the velocity vanishes at the midpoint $z = L$ between the P vessels. This half-width L of the s vessel arcade can also be viewed as a characteristic length reflecting the rate of capillary bleed off from the s vessels. Thus, changing L can show us the effect of the bleed off on the local heat transfer. The effect of L on the axial thermal equilibration length of the artery is illustrated in Fig. 5 for different blood

flow rates, Pe_a = 5 (resting state), 25 (moderate flow), 50 (exercise) for mean representative values of R_t and l. The artery thermal equilibration length is the distance over which the artery bulk temperature decreases by a factor of e. This figure also compares the thermal equilibration lengths with and without capillary bleed off and the light lines (with bleed off), Eq. (21), will approach the heavy lines (without bleed off), Eq. (23), when L is infinity. From the data in Table 1 the most likely range of L is from 150 to 250. Increasing L for a constant inflow Pe_a is equivalent to decreasing the capillary bleed off rate per unit cylinder length. At the lower capillary bleed off rates (larger L) the thermal equilibration length is found to be almost proportional to the inflow Peclet number and the thermal equilibration length is a weak function of the rate of capillary bleed off. At high flow conditions (Pe_a = 50) increasing L greatly increases the thermal equilibration length, whereas at low flow conditions, the axial thermal equilibration is almost unchanged since blood flow in the vessels contributes little to the axial thermal interaction.

The theoretically predicted temperature profiles in the center plane $y = 0$ of the countercurrent vessel pair are shown in Fig. 6 for two vessel center-to-center spacings, l = 2 and 6. The temperature profiles have a similar shape at all values of z, but the peak temperature decays with axial distance as shown in Fig. 4. In this figure, the artery and the vein are symmetrically located on the left and the right side of the x axis so that $l = 2s_s = 2s_v$. One notes that the maximum and minimum points are located inside the artery and vein, respectively, and due to the countercurrent rewarming there is no sharp minimum for the vein.

We have examined the effects of several factors on the venous return temperature T_{vb0} and the correction coefficient ΔT in Eqs. (24) and (25). Please note that the larger ΔT, the lower the venous return temperature. The dependence of ΔT on the tissue cylinder radius is shown in Fig. 7 for several center-to-center spacings. When the ratio of the cylinder radius to the artery radius, R_t, is less than 50, the maximum dimensionless venous return temperature that can be achieved is found to be 0.45 ($\Delta T > 0.55$). Thus, even for the touching configuration (l = 2) more than half of the heat leaving the artery is lost to the outer boundary of the tissue cylinder and, therefore, it is hard to rewarm the countercurrent vein. Obviously, a change in the tissue cylinder size leads to a change in the conduction resistance between the countercurrent vessel pair and the tissue cylinder outer boundary. Increasing R_t causes a decrease in ΔT since more heat leaving the artery eventually will return to rewarm the countercurrent vein rather than being lost to the tissue cylinder. Eventually, when R_t approaches infinity, perfect countercurrent heat exchange will be achieved so that ΔT will approach zero. However, it is clear from Fig. 7 that this occurs for $R_t \gg 50$. It is also observed that when the ratio of the vessel spacing to the cylinder diameter l/R_t is larger than 0.75, more than 90 percent of the heat leaving the artery will be lost to the tissue cylinder, i.e., $\Delta T > 0.9$. Under these conditions the original Pennes equation is a good approximation for the perfusion source term. Since l/R_t lies primarily in the range 0.05 to 0.4, this occurs only at the largest spacing of the s vessel pair, l = 6, and values of $R_t < 8$.

Figure 8 shows how the vessel center-to-center spacing (l) influences ΔT for the case of equal and unequal sized vessels symmetrically positioned relative to the tissue cylinder center for a representative R_t of 20. One notes that ΔT decreases substantially due to the effect of countercurrent heat exchange as l approaches 2, the touching configuration, where ΔT has the limiting value of 0.61. Countercurrent heat exchange is an important consideration for s vessel spacings in the most frequently observed range from 2.5 to 3.0 where the theory predicts that 30 to 40 percent of the heat leaving the s artery is recaptured by the s vein. The influence of the unequal vessel size case is also shown in Fig. 8, for the case where the returning s vein is twice the size of the artery. The effect of unequal vessel size is small and produces less than a 4 percent variation in the correction coefficient ΔT since the thermal resistance within each vessel is a small fraction of the total thermal resistance between the two vessels. The region bounded by the curves $a_v^*/a_a^* = 1$ and 2 and l = 2.5 to 3 is representative of most of the tissues in Table 1.

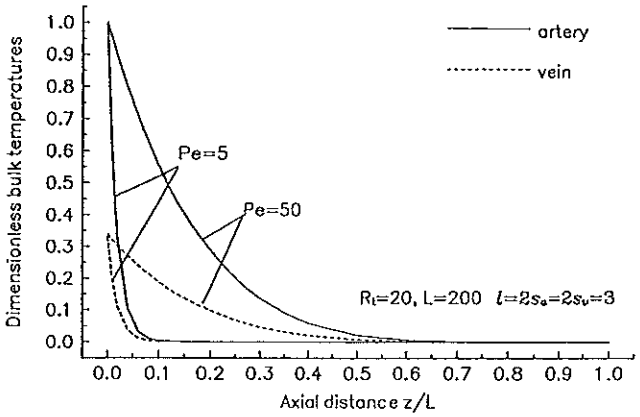

Fig. 4 The effect of blood flow Peclet number on the axial temperature distribution

Table 1 Geometric parameters in muscle tissue cylinder

Muscle type	Radius of the primary artery (μm)	Radius of the secondary artery (a_a^*) (μm)	Radius of the terminal arteriole (μm)	Cylinder radius (R_t^*)	Half length of tissue cylinder (L^*) (mm)	R_t
Tenuissumus	40-63	30-38	10-15	560*	6.2	14-18
Biceps femoris	63-133	25-40	15-28	920	------	23-36
Gastrocnemius (lateral head)	108-173	35-45	18-20	940	------	20-26
Gastrocnemius (media head)	80-155	30-50	15-25	614	------	12-20
Soleus	90-193	25-55	13-23	444	------	8-17
Extensor Hallucis Proprius Muscle	------	~25	4-6	400*	6.5	~16

* equivalent radius

7 Discussion

In this study, a new analysis for the perfusion source term in the tissue energy equation has been developed to describe

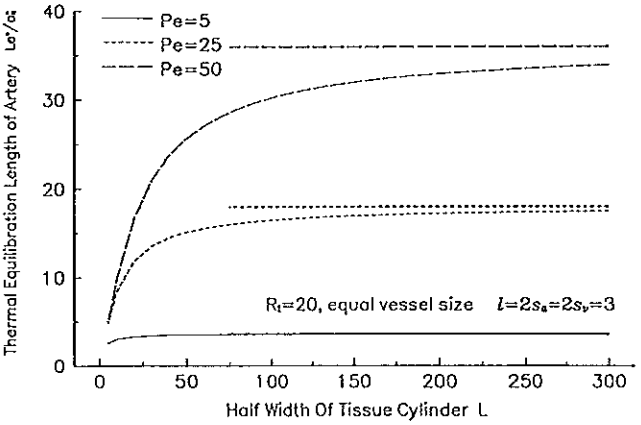

Fig. 5 The effect of L on the axial thermal equilibration length of the artery. Values with and without capillary bleed off are shown by the light lines and heavy lines, respectively.

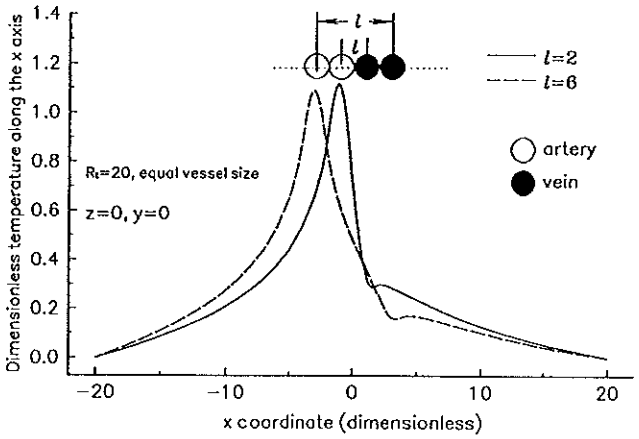

Fig. 6 The temperature profiles in the vicinity of the countercurrent vessel pair

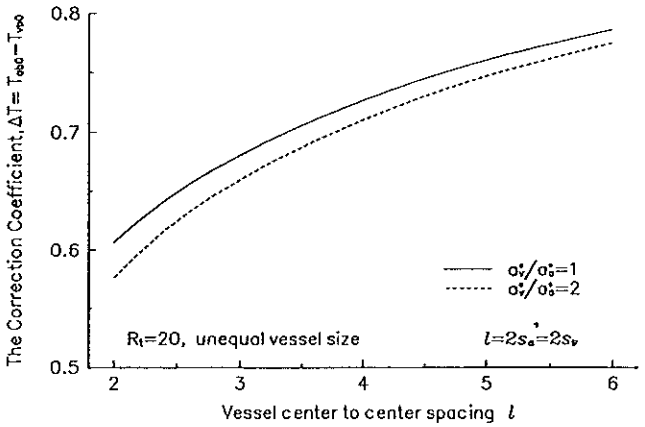

Fig. 8 Correction coefficient ΔT as a function of vessel center to center spacing l for the cases of equal and unequal sized vessels

the effect of blood perfusion on local tissue heat transfer based on a detailed anatomical analysis of the microvascular bed in a muscle tissue cylinder identified by Myrhage and Eriksson as the basic structural unit that is common to most skeletal muscle tissue. The results of this study show that the effect of the blood perfusion over a wide range of conditions can be accurately evaluated by analyzing the countercurrent heat exchange between the s vessels in this muscle tissue cylinder. The derivation in this paper differs from other theoretical models [3–5, 7, 10, 33] in that it provides the first rational model based on the actual anatomical structure of muscle for determining the local venous return temperature. A closed-form solution is obtained for the temperature field in both the tissue and vessel regions using a rigorous asymptotic analysis of the vascular and tissue cylinder geometry. In contrast to most previous theoretical models for countercurrent heat exchange, the model allows the vessel wall temperature to be nonuniform, accounts for capillary bleed off, and makes no a priori assumption as to the blood flow Nusselt number.

The newly derived perfusion source term reflects the thermal importance of both the capillary bleed off and countercurrent heat exchange mechanisms. Countercurrent convective heat exchange becomes more important relative to the capillary bleed off when the countercurrent vessels are closely spaced and $R_t \gg 1$. This results in a higher value of the venous return temperature or lower value of the correction coefficient ΔT. In contrast, most of the heat leaving the artery is lost to the tissue for large s, l and small R_t and the original Pennes source term is a good approximation for $l/R_t > 0.75$. However, this value of l/R_t is not realistic for the most tissues, where l/R_t is close to 0.1, and there is typically a 30 to 55 percent countercurrent rewarming of the vein. Our previous theoretical and experimental study of axial thermal equilibration in exteriorized rat cremaster muscle preparations [38] showed a significantly greater countercurrent rewarming (>80 percent) of the countercurrent vein. The important difference is that in the two-dimensional tissue preparations, the heat resistance between the countercurrent vessel pair and the tissue included not only the conductive resistance of the tissue but also the convective resistance of the air at the preparation surface. The latter is much larger than the former so that the air surrounding the preparation acts like an insulator, which prevents the heat leaving the feeding artery from being lost to the external environment. A higher venous return temperature is, therefore, expected in an exteriorized tissue preparation. The blood perfusion can act as either a heat sink or source depending on the temperature difference between the local arterial supply temperature and the local average tissue temperature. Under normal conditions, the arterial temperature is higher than the surrounding tissue temperature so that the blood perfusion acts like a heat source, while under hyperthermic conditions, the perfusion might act as a heat sink within the heated tissue region.

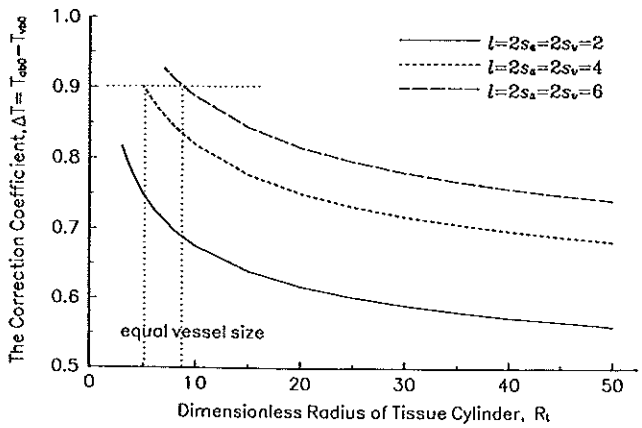

Fig. 7 Correction coefficient ΔT as a function of tissue cylinder radius R_t for various vessel center-to-center spacings l, $l = 2s_a = 2s_v$.

One surprising result is that, in contrast to the results of Brinck and Werner [8], the correction coefficient ΔT depends only on the local vascular and tissue cylinder geometry and is independent of the local perfusion rate when there is equal flow in the s vessel pair. Therefore, it is the s vessel cylinder geometry rather than the blood flow rate that determines the strength of the perfusion source term. The blood flow rate influences only the axial thermal equilibration length, while the vascular geometry in the cross-sectional plane determines the thermal resistance between the vessel pair and the tissue. This behavior is the consequence of three assumptions used in the model: (*i*) The countercurrent heat exchange is the only driving force for the heat transfer, (*ii*) the flow vanishes at the midpoint of the tissue cylinder and the artery and the vein temperatures are equal to the local tissue temperature at this point, and (*iii*) the same mass flow is assumed in each vessel of the s vessel pair. This behavior is similar to that obtained by Baish et al. [4], where in the limit of long equilibration lengths, the governing equations for the countercurrent model resemble the Pennes equation and the strength of the heat sink is determined by the geometry of the model, not the flow rate. As shown in Zhu et al. [38], in the limit of long equilibration lengths, axial conduction can be neglected and the countercurrent flow becomes the dominant driving force for thermal equilibration. Only when both the flow rate is low and there is a large temperature gradient

along the axial direction does axial conduction become comparable to or larger than countercurrent heat exchange. In this analysis we have assumed that the muscle tissue cylinder is parallel to the skin surface and the tissue temperature gradients in this direction are negligible.

In Chato [11] and Baish's [2] analyses, the effectiveness of the countercurrent heat exchange is based on an isolated countercurrent vessel pair in an infinite medium not a finite tissue cylinder. The thermal "effectiveness" defined in Chato's paper ($\epsilon = (E + N_0)/(1 + N_0)$) can vary from 0 to 1 and is strongly affected by the values of both N_0 (reference number of heat transfer unit, UA/m_0c_0) and E (mass transfer fraction between vessels). A lower overall heat transfer coefficient (UA), which may be caused by smaller vessel spacing, can result in a warmer venous return blood flow. This conclusion is consistent with our results. However, a larger blood flow or smaller capillary bleed off rate can result in less heat transfer between vessels and thus a lower venous return temperature in Chato's model, while our correction coefficient is independent of blood flow and capillary bleed off rate. This is due to the flow geometry and boundary conditions of our muscle tissue cylinder. If one requires that the blood flow vanish at $z = L$ into Chato's model, i.e., $E = 1$, one finds that the effectiveness is equal to 1 and independent of blood flow as in our model. This similar behavior is expected since axial conduction is neglected in both models. Brinck and Werner [8] used parameter fitting to determine the value of the "effectiveness" of the perfusion term as a function of blood flow. The artery temperature variation was not considered and no closed-form analytic expression was given in their analysis. The efficiency function derived by Brinck and Werner [8] is based on averaging the heat and mass transport equations over the whole limb. The perfusion-dependent efficiency functions obtained in their model as a result of curve fitting describe the combined effects of both perfusion and artery temperature variations in the limb, which are strongly influenced by vessel size, presence or absence of local heating, and the blood perfusion rate.

In this paper, the correction coefficient is derived for normal resting conditions. The total thermal interaction between countercurrent vessels and the local tissue can be affected by any heat source introduced into the tissue region, such as hyperthermia, metabolism, etc. These heat sources will change the results significantly only if the axial thermal gradients produced are significant on the length scale of the half length of the s vessel tissue cylinder, ~6 mm. In the new model only the last five to six generations of branching in the Weinbaum–Jiji anatomical description have been replaced by the much more efficient description of the s vessel tissue cylinder. The important remaining unknown in our modified Pennes equation, Eq. (25), is the local arterial inlet temperature T_{ab0}. This temperature is determined by the thermal interaction in the SAV supply vessels after they branch off from the central supply vessels that run along the axis of the limb. In fact both the P vessels and the SAV vessels can be considered as part of the thermally significant feeding vessel system that lies upstream of the s vessel tissue cylinders. The temperature of the tissue surrounding the SAV vessel pair will in general vary as one proceeds toward the peripheral tissue layer. This basic problem will be addressed in part II of the present study [40]. In principle, in treating an entire limb one would like to derive general results for these larger vessels and not have to treat them individually. Crezee et al. [15] have suggested a different approach. Vessels >300 μm in diameter are treated discretely and vessels <300 μm in diameter are modeled as a continuum thermal source.

Acknowledgments

This research was supported by CUNY collaborative incentive Grant Program award #9-91959 to Lisa X. Xu, Sheldon Weinbaum, and Daniel E. Lemons.

References

1 Anderson, G. T., and Valvano, J. W., 1994, "A Small Artery Heat Transfer Model for Self-Heated Thermistor Measurements of Perfusion in the Kidney Cortex," ASME JOURNAL OF BIOMECHANICAL ENGINEERING, Vol. 116, pp. 71–78.

2 Baish, J. W., 1994, "Formulation of a Statistical Model of Heat Transfer in Perfused Tissue," ASME JOURNAL OF BIOMECHANICAL ENGINEERING, Vol. 116, pp. 521–527.

3 Baish, J. W., 1990, "Heat Transfer by Countercurrent Blood Vessels in the Presence of an Arbitrary Temperature Gradient," ASME JOURNAL OF BIOMECHANICAL ENGINEERING, Vol. 112, pp. 207–213.

4 Baish, J. W., Ayyaswamy, P. S., and Foster, K. R., 1986, "Heat Transport Mechanism in Vascular Tissues: a Model Comparison," ASME JOURNAL OF BIOMECHANICAL ENGINEERING, Vol. 108, pp. 324–331.

5 Baish, J. W., Ayyaswamy, P. S., and Foster, K. R., 1986, "Small-Scale Temperature Fluctuations in Perfused Tissue During Local Hyperthermia," ASME JOURNAL OF BIOMECHANICAL ENGINEERING, Vol. 108, pp. 246–250.

6 Bjornberg, J., Grande, P. O., Maspers, M., and Mellander, S., 1988, "Site of Autoregulatory Reactions in the Vascular Bed of Cat Skeletal Muscle as Determined With a New Technique for Segmental Vascular Resistance Recordings," *Acta Physiol. Scand.*, Vol. 133, pp. 199–210.

7 Brinck, H., and Werner, J., 1994, "Estimation of the Thermal Effect of Blood Flow in a Branching Countercurrent Network Using a Three-Dimensional Vascular Model," ASME JOURNAL OF BIOMECHANICAL ENGINEERING, Vol. 116, pp. 324–330.

8 Brinck, H., and Werner, J., 1994, "Efficiency Function: Improvement of Classical Bioheat Approach," *Journal of Applied Physiology*, Vol. 77(4), pp. 1617–1622.

9 Charny, C. K., 1992, "Mathematical Models of Bioheat Transfer," in: *Advances in Heat Transfer*, Vol. 22, Y. I. Cho, ed., Academic Press, Boston, pp. 19–155.

10 Charny, C. K., Weinbaum, S., and Levin, R. L., 1990, "An Evaluation of the Weinbaum–Jiji Bioheat Equation for Normal and Hyperthermic Conditions," ASME JOURNAL OF BIOMECHANICAL ENGINEERING, Vol. 112, pp. 80–87.

11 Chato, J., 1980, "Heat Transfer to Blood Vessels," ASME JOURNAL OF BIOMECHANICAL ENGINEERING, Vol. 102, pp. 110–118.

12 Chen, M. M., and Holmes, K. K., 1980, "Microvascular Contributions to Tissue Heat Transfer," *Annals of the NY Acad. of Science*, Vol. 335, pp. 137–150.

13 Crezee, J., Mooibroek, J., Lagendijk, J. J. W., and Van Leneuwen, G. M. J., 1994, "The Theoretical and Experimental Evaluation of the Heat Balance in Perfused Tissue," *Phys. Med. Biol.*, Vol. 39, pp. 813–832.

14 Crezee, J., Mooibroek, J., Bos, C. K., and Lagendijk, J. J. W., 1991, "Interstitial Heating: Experiments in Artificially Perfused Bovine Tongues," *Phys. Med. Biol.*, Vol. 36, pp. 823–833.

15 Crezee, J., and Lagendijk, J. J. W., 1990, "Experimental Verification of Bioheat Transfer Theories: Measurement of Temperature Profiles around Large Artificial Vessels in Perfused Tissue," *Phys. Med. Biol.*, Vol. 35(7), pp. 905–923.

16 Dagan, Z., Weinbaum, S., and Pfeffer, R., 1982, "An Infinite-Series Solution for the Creeping Motion Through an Orifice of Finite Length," *J. Fluid Mech.*, Vol. 115, pp. 505–523.

17 Eriksson, E., and Myrhage, R., 1972, "Microvascular Dimensions and Blood Flow in Skeletal Muscle," *Acta Physiol. Scand.*, Vol. 86, pp. 211–222.

18 Jiji, L. M., Weinbaum, S., and Lemons, D. E., 1984, "Theory and Experiment for the Effect of Vascular Microstructure on Surface Tissue Heat Transfer. Part II—Model Formulation and Solution," ASME JOURNAL OF BIOMECHANICAL ENGINEERING, Vol. 106, pp. 331–341.

19 Lemons, D. E., Chien, S., Crawshaw, L. I., Weinbaum, S., and Jiji, L. M., 1987, "The Significance of Vessel Size and Type in Vascular Heat Transfer," *Am. J. Physiol.*, Vol. 253, pp. R128–R135.

20 Pennes, H. H., 1948, "Analysis of Tissue and Arterial Blood Temperatures in the Resting Human Forearm," *J. Applied Physiology*, Vol. 1, pp. 93–122.

21 Maspers, M., Bjornberg, J., Grande, J. P. O., and Mellander, O., 1989, "Sympathetic α-adrenergic Control of Larger-Bore Arterial Vessels, Arterioles and Veins, and of Capillary Pressure and Fluid Exchange in Whole Organ Cat Skeletal Muscle," *Acta Physiol. Scand.*, Vol. 138, pp. 509–521.

22 Myrhage, R., 1977, "Microvascular Supply of Skeletal Muscle Fibers: a Microangiographic, Histochemical and Intravital Microscopic Study of Hind Limb Muscles in the Rat, Rabbit and Cat," *Acta Orthop. Scand.*, Vol. 168, pp. 1–46.

23 Myrhage, R., and Eriksson, E., 1984, "Arrangement of the Vascular Bed in Different Types of Skeletal Muscles," *Prog. Appl. Microcirc.*, Vol. 5, pp. 1–14.

24 Myrhage, R., and Eriksson, E., 1980, "Vascular Arrangement in Hind Limb Muscles of the Cat," *J. Anatomy*, Vol. 131(1), pp. 1–17.

25 Myrhage, R., and Hudlicka, O., 1976, "The Microvascular Bed and Capillary Surface Area in Rat Extensor Hallucis Proprius Muscle (EHP)," *Microvascular Research*, Vol. 11, pp. 315–323.

26 Roemer, R. B., Moros, E. G., and Hynynen, K., 1989, "A Comparison of Bioheat Transfer and Effective Conductivity Equation Predictions to Experimental Hyperthermia Data," *Adv. Bioeng.*, ASME WAM, pp. 11–15.

27 Valvano, J. W., Nho, S., and Anderson, G. T., 1994, "Analysis of the Weinbaum–Jiji Model of Blood Flow in the Canine Kidney Cortex for Self-Heated Thermistors," ASME JOURNAL OF BIOMECHANICAL ENGINEERING, Vol. 116, pp. 201–207.

28 Weinbaum, S., Jiji, L. M., and Lemons, D. E., 1992, "The Bleed Off Perfusion Term in the Weinbaum–Jiji Bioheat Equation," ASME JOURNAL OF BIOMECHANICAL ENGINEERING, Vol. 114, pp. 539–542.
29 Weinbaum, S., and Lemons, D. E., 1992, "Heat Transfer in Living Tissue: the Search for a Blood–Tissue Energy Equation and the Local Thermal Microvascular Control Mechanism," *BMES Bull.*, Vol. 16(3), pp. 38–43.
30 Weinbaum, S., and Jiji, L. M., 1989, "The Matching of Thermal Fields Surrounding Countercurrent Microvessels and the Closure Approximation in the Weinbaum–Jiji Bioheat Equation," ASME JOURNAL OF BIOMECHANICAL ENGINEERING, Vol. 111, pp. 271–275.
31 Weinbaum, S., and Jiji, L. M., 1987, "Discussion of Papers by Wissler and Baish et al. Concerning the Weinbaum–Jiji Bioheat Equation," ASME JOURNAL OF BIOMECHANICAL ENGINEERING, Vol. 109, pp. 234–237.
32 Weinbaum, S., and Jiji, L. M., 1985, "A New Simplified Bioheat Equation for the Effect of Blood Flow on Local Average Tissue Temperature," ASME JOURNAL OF BIOMECHANICAL ENGINEERING, Vol. 107, pp. 131–139.
33 Weinbaum, S., Jiji, L. M., and Lemons, D. E., 1984, "Theory and Experiment for the Effect of Vascular Microstructure on Surface Tissue Heat Transfer—Part I: Anatomical Foundation and Model Conceptualization," ASME JOURNAL OF BIOMECHANICAL ENGINEERING, Vol. 106, pp. 321–330.
34 Wissler, E. H., 1988, "Comments on the New Bioheat Equation Proposed by Weinbaum and Jiji," ASME JOURNAL OF BIOMECHANICAL ENGINEERING, Vol. 109, pp. 226–233.
35 Wissler, E. H., 1987, "Comments on Weinbaum and Jiji's discussion of their proposed bioheat equation," ASME JOURNAL OF BIOMECHANICAL ENGINEERING, Vol. 109, pp. 355–356.
36 Wu, Y. L., Weinbaum, S., Jiji, L. M., and Lemons, D. E., 1993, "A New Analytic Technique for 3-D Heat Transfer From a Cylinder With Two or More Axially Interacting Eccentrically Embedded Vessels With Application to Countercurrent Blood Flow," *Int. J. Heat Mass Transfer*, Vol. 36, pp. 1073–1083.
37 Xu, L. X., Chen, M. M., Holmes, K. R., and Arkin, H., 1991, "The theoretical evaluation of the Pennes, the Chen-Holmes and the Weinbaum–Jiji bioheat transfer models in the pig renal cortex," ASME HTD-Vol. 189, pp. 15–22.
38 Zhu, L., Lemons, D. E., and Weinbaum, S., 1996, "Microvascular Thermal Equilibration in Rat Cremaster Muscle," *Annals of Biomedical Engineering*, Vol. 24, pp. 109–123.
39 Zhu, L., Lemons, D. E., and Weinbaum, S., 1995, "A New Approach for Prediction the Enhancement in the Effective Conductivity of Perfused Muscle Tissue Due to Hyperthermia," *Annals of Biomedical Engineering*, Vol. 23, pp. 1–12.
40 Zhu, L., Xu, L. X., and Weinbaum, S., "A New Fundamental Bioheat Equation for Muscle Tissue, Part II: Temperature of SAV Vessels," in preparation.
41 Zhu, M., Weinbaum, S., and Jiji, L. M., 1990, "Heat Exchange Between Unequal Countercurrent Vessels Asymmetrically Embedded in a Cylinder With Surface Convection," *Int. J. Heat Mass Transfer*, Vol. 33, pp. 2275–2284.

APPENDIX

In this appendix we derive the expressions for the radial and axial velocity components in an artery with porous walls. The governing equations for the axisymmetric flow are

Continuity:

$$\frac{\partial u_a^*}{\partial z^*} + \frac{1}{r_a^*}\frac{\partial (r_a^* v_a^*)}{\partial r_a^*} = 0 \tag{A.1}$$

Momentum:

$$\begin{cases} u_a^*\dfrac{\partial u_a^*}{\partial z} + v_a^*\dfrac{\partial u_a^*}{\partial r_a^*} = -\dfrac{1}{\rho_f}\dfrac{\partial p^*}{\partial z^*} \\ \qquad + v_f\left[\dfrac{1}{r_a^*}\dfrac{\partial}{\partial r_a^*}\left(r_a^*\dfrac{\partial u_a^*}{\partial r_a^*}\right) + \dfrac{\partial^2 u_a^*}{\partial z^{*2}}\right] \end{cases} \tag{A.2}$$

$$\begin{cases} u_a^*\dfrac{\partial v_a^*}{\partial z} + v_a^*\dfrac{\partial v_a^*}{\partial r_a^*} = -\dfrac{1}{\rho_f}\dfrac{\partial p^*}{\partial r_a^*} \\ \qquad + v_f\left[\dfrac{1}{r_a^*}\dfrac{\partial}{\partial r_a^*}\left(r_a^*\dfrac{\partial v_a^*}{\partial r_a^*}\right) + \dfrac{\partial^2 v_a^*}{\partial z^{*2}} - \dfrac{v_a^*}{r_a^{*2}}\right] \end{cases} \tag{A.3}$$

where v_f is the kinematic viscosity of the blood. The nondimensionalization of these equations is performed by first introducing characteristic quantities that scale the dimensional variables and make them of O(1):

$$r_a = \frac{r_a^*}{a_a^*},\ z = \frac{z^*}{L^*},\ u_a = \frac{u_a^*}{u_{a0}^*},\ v_a = \frac{v_a^*}{u_{a0}^* a_a^*/L^*},\ p = \frac{p^*}{\rho_f u_{a0}^{*2}}$$

If the dimensionless variables just defined are introduced into the governing equations, Eqs. (A.2) and (A.3) become

$$\begin{cases} \dfrac{a_a^* \mathrm{Re}_a}{L^*}\left[u_a\dfrac{\partial u_a}{\partial z} + v_a\dfrac{\partial u_a}{\partial r_a}\right] \\ \qquad = -\mathrm{Re}_a\dfrac{\partial p}{\partial z} + \dfrac{\partial}{\partial r_a}\left(r_a\dfrac{\partial u_a}{\partial r_a}\right) + \dfrac{a_a^{*2}}{L^{*2}}\dfrac{\partial^2 u_a}{\partial z^2} \end{cases} \tag{A.4}$$

$$\begin{cases} \dfrac{a_a^{*2}}{L^{*2}}\left[u_a\dfrac{\partial v_a}{\partial z} + v_a\dfrac{\partial v_a}{\partial r_a}\right] = -\dfrac{\partial p}{\partial r_a} + \dfrac{a_a^*}{\mathrm{Re}_a L^*}\dfrac{\partial}{\partial r_a}\left(r_a\dfrac{\partial v_a}{\partial r_a}\right) \\ \qquad + \dfrac{a_a^{*3}}{\mathrm{Re}_a L^{*3}}\dfrac{\partial^2 v_a}{\partial z^2} - \dfrac{a_a^*}{\mathrm{Re}_a L^* r_a^2}\dfrac{v_a}{} \end{cases} \tag{A.5}$$

The Reynold number, $\mathrm{Re}_a = a_a^* u_a^*/v_f$ for a typical 50 μm artery varies between 0.5 (resting state) to 5 (heavy exercise) and the parameter L^*/a_a^* is approximately equal to 200. Examination of these equations reveals that the terms with the coefficient $a_a^*\mathrm{Re}_a/L^*$ or $a_a^*/L^*\mathrm{Re}_a$ are of lower order in these equations. Therefore, if these terms are neglected, one can rewrite the original dimensional Eqs. (A.2) and (A.3) as

$$\frac{1}{\rho_f}\frac{\partial p^*}{\partial z^*} = \frac{v_f}{r_a^*}\frac{\partial}{\partial r_a^*}\left(r_a^*\frac{\partial u_a^*}{\partial r_a^*}\right) \tag{A.6}$$

$$\frac{\partial p^*}{\partial r_a^*} = 0 \tag{A.7}$$

At the Re_a considered herein Eqs. (A.6) and (A.7) apply downstream of a short entrance region that is at most two vessel diameters, see [16], where a quasi fully developed velocity profile is achieved. For a vessel 100 μm in diameter this is at most 3 percent of the half length of s vessel tissue cylinder.

Equation (A.7) requires constant pressure in the cross-sectional plane so that the term, $\partial p^*/\partial z^*$, can be written as dp^*/dz^*. The assumption of a constant bleed off from the s vessels suggests an expression of the form

$$u_a^* = (1 - z^*/L^*) f(r_a^*)$$

where $f(r_a^*)$ is a function of r_a^*. Substituting this form back into Eq. (A.6), one finds that the pressure gradient must be proportional to $(1 - z^*/L^*)$. Integrating Eq. (A.6) twice, satisfying the no-slip condition on u_a^* at $r_a^* = a_a^*$ and introducing the average velocity at $z = 0$, u_{a0}^*, one obtains the solution for u_a^*, which is given by

$$u_a^* = 2u_{a0}^*(1 - z^*/L^*)(1 - r_a^{*2}/a_a^{*2})$$

The velocity in the radial direction v_a^* is determined by the requirement of flow continuity. Substituting the expression for u_a^* into Eq. (A.1) and integrating this equation, one obtains

$$v_a^* = u_{a0}^*\frac{a_a^*}{L^*}\left(\frac{r_a^*}{a_a^*} - \frac{r_a^{*3}}{2a_a^{*3}}\right)$$

These results are Eqs. 2(a) and 2(b) in the main text.